Available online at www.sciencedirect.com
ScienceDirect
Journal of Sound and Vibration 321 (2009) 242–253
JOURNAL OF SOUND AND VIBRATION
www.elsevier.com/locate/jsvi

Electrically forced vibration of an elastic plate with a finite piezoelectric actuator

Zengtao Yang[a], Shaohua Guo[a], Jiashi Yang[a,b,*], Yuantai Hu[c]

[a]*Institute of Mechanics and Sensing Technology, School of Civil Engineering and Architecture, Central South University, Changsha, Hunan 410083, China*
[b]*Department of Engineering Mechanics, University of Nebraska, Lincoln, NE 68588-0526, USA*
[c]*Department of Mechanics, Huazhong University of Science and Technology, Wuhan, Hubei 430074, China*

Received 4 January 2008; received in revised form 26 August 2008; accepted 18 September 2008
Handling Editor: S. Bolton
Available online 25 October 2008

Abstract

We analyze out-of-plane vibrations of an elastic plate electrically driven by a finite piezoelectric actuator on part of the surface of the plate. The equations of linear elasticity and linear piezoelectricity are used. The mathematical problem is solved using trigonometric series. An exact solution satisfying all governing equations and boundary conditions is obtained. Basic vibration characteristics including resonant frequencies, mode shapes and electric admittance are calculated. It is shown that the vibration may be either confined to the actuator region or all over the plate, and the vibration behavior is sensitive to the parameters of the structure.

1. Introduction

An elastic plate with piezoelectric layers has been studied extensively for smart structural applications, e.g., Refs. [1–7]. These analyses usually focus on the so-called low-frequency modes of flexure or extension. The frequencies of these modes are strongly dependent on the plate length or width. In smart structural analyses, approximate two-dimensional plate theories and accompanying numerical methods are often used. An elastic plate with a piezoelectric layer attached is also a fundamental structure for many applications including acoustic wave devices and nondestructive evaluation. In these applications, in addition to the low-frequency modes, the so-called high-frequency modes like thickness-extensional, thickness-shear and thickness-twist are also used. The frequencies of these modes are mainly determined by the plate thickness. When the piezoelectric layer(s) covers the entire elastic plate, exact analyses are possible for plates with simple geometry, e.g., rectangular plates [8–12]. The situation when the elastic plate is only partially covered by a piezoelectric patch is also very useful but from the modeling point of view it represents a much more complicated problem and is usually analyzed approximately [13–16]. Specifically, for the so-called anti-plane

*Corresponding author at: Department of Engineering Mechanics, University of Nebraska, Lincoln, NE 68588-0526, USA.
E-mail address: jyang1@unl.edu (J. Yang).

0022-460X/$ - see front matter © 2008 Elsevier Ltd. All rights reserved.
doi:10.1016/j.jsv.2008.09.032

(out-of-plane) or shear horizontal motions, the problem of a finite piezoelectric patch on an elastic half-space was analyzed in Ref. [17]. This problem is fundamental to various applications. In this paper we study a more practical situation in which the elastic substrate is a plate. Compared to a half-space, a plate has more boundaries and therefore making the problem more challenging. A trigonometric series approach is used in our analysis which allows us to obtain a solution satisfying the equations of elasticity and piezoelectricity.

2. Structure

Consider the structure in Fig. 1. The elastic plate is isotropic and is of length $a+b$ and thickness $2h$. The piezoelectric transducer is of length $2L$ and thickness $2h'$. The structure is infinitely long in the x_3 direction determined from the x_1 and x_2 axes by the right-hand rule. The transducer is made from polarized ceramics with the poling direction along the x_3 axis. The transducer is electroded at its top and bottom surfaces, with the electrodes shown by the thick lines. The electrodes are very thin. Their mechanical effects like inertia and stiffness are negligible. What the electrodes do is that they provide electrical constraints on the electric potential which is a constant on an electrode. The transducer is under a driving voltage $2V$ which later will be assumed time-harmonic. The elastic plate is a dielectric (insulator). If a metal plate is considered, a very thin insulating layer is assumed between the bottom electrode of the transducer and the elastic plate.

3. Governing equations

For the material orientation and electrode configuration in Fig. 1, the transducer and elastic plate can be electrically excited into shear horizontal (SH) modes with

$$u_1 = u_2 = 0, \quad u_3 = u(x_1, x_2, t). \tag{1}$$

3.1. Equations for the elastic plate

For the isotropic elastic plate, the nonzero components of the strain S_{ij} and stress T_{ij} are

$$S_4 = 2S_{32} = u_{,2}, \quad S_5 = 2S_{31} = u_{,1},$$

$$T_4 = \mu u_{,2}, \quad T_5 = \mu u_{,1}, \tag{2}$$

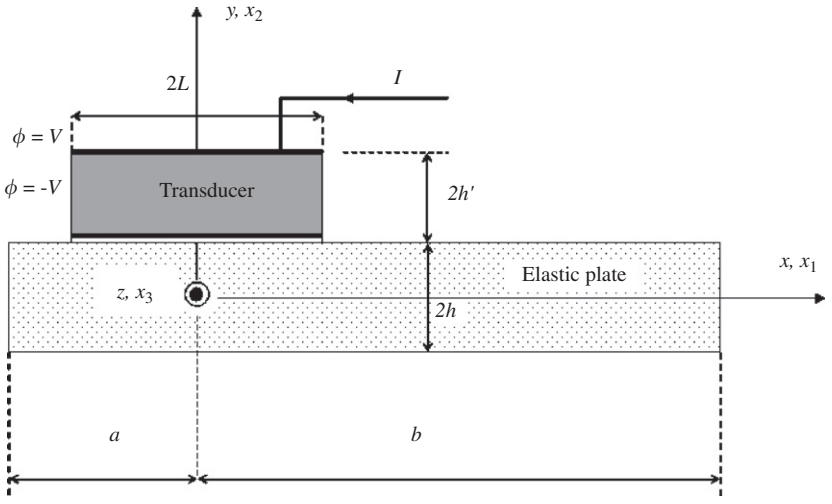

Fig. 1. An elastic plate with a finite piezoelectric actuator.

where μ is the shear elastic constant and the subscript ,1 denotes differentiation with respect to x_1, etc. The nontrivial equation of motion takes the following form:

$$c_2^2\nabla^2 u = \ddot{u}, \tag{3}$$

where $\nabla^2 = \partial_1^2 + \partial_2^2$ is the two-dimensional Laplacian. c_2 is the speed of plane shear waves given by

$$c_2^2 = \mu/\rho_1, \tag{4}$$

where ρ_1 is the mass density.

3.2. Equations for the transducer

For ceramics poled in the x_3 direction, corresponding to the displacement field in Eq. (1), there exists an electric potential of the following form [18,19]:

$$\phi = \phi(x_1, x_2, t). \tag{5}$$

The nonzero strain and electric field components are

$$\begin{Bmatrix} 2S_{13} \\ 2S_{23} \end{Bmatrix} = \nabla u, \quad \begin{Bmatrix} E_1 \\ E_2 \end{Bmatrix} = -\nabla\phi, \tag{6}$$

where $\nabla = \mathbf{i}_1\partial_1 + \mathbf{i}_2\partial_2$ is the two-dimensional gradient operator. $\mathbf{E}$ is the electric field. The nontrivial components of T_{ij} and the electric displacement D_i are

$$\begin{Bmatrix} T_{13} \\ T_{23} \end{Bmatrix} = c\nabla u + e\nabla\phi, \quad \begin{Bmatrix} D_1 \\ D_2 \end{Bmatrix} = e\nabla u - \varepsilon\nabla\phi, \tag{7}$$

where we have denoted the relevant elastic, piezoelectric and dielectric constants by $c = c_{44}$, $e = e_{15}$ and $\varepsilon = \varepsilon_{11}$. The nontrivial equation of motion and the charge equation of electrostatics take the following form:

$$c\nabla^2 u + e\nabla^2\phi = \rho\ddot{u}, \quad e\nabla^2 u - \varepsilon\nabla^2\phi = 0. \tag{8}$$

We introduce [18,19]

$$\psi = \phi - \frac{e}{\varepsilon}u. \tag{9}$$

Then, in terms of u and ψ,

$$T_{23} = \bar{c}u_{3,2} + e\psi_{,2}, \quad T_{31} = \bar{c}u_{3,1} + e\psi_{,1},$$

$$D_1 = -\varepsilon\psi_{,1}, \quad D_2 = -\varepsilon\psi_{,2}, \tag{10}$$

and

$$v_T^2\nabla^2 u = \ddot{u}, \quad \nabla^2\psi = 0, \tag{11}$$

where

$$v_T^2 = \frac{\bar{c}}{\rho}, \quad \bar{c} = c + \frac{e^2}{\varepsilon} = c(1+k^2), \quad k^2 = \frac{e^2}{\varepsilon c}. \tag{12}$$

To calculate the charge Q and current I on the upper electrode as well as the admittance Y of the transducer, we need

$$Q = \int_{-L}^{L} -D_2|_{y=h+2h'}\,\mathrm{d}x,$$

$$I = \dot{Q}_1 = \mathrm{i}\omega Q_1 = Y2V, \tag{13}$$

where a unit dimension in the x_3 direction is considered.

3.3. Boundary and continuity conditions

At the top and bottom surfaces as well as the interface we have

$$\phi(h+2h') = V, \quad |x|<L,$$

$$T_{23}(h+2h') = 0, \quad |x|<L,$$

$$\phi(h^+) = -V, \quad |x|<L,$$

$$u(h^-) = u(h^+), \quad |x|<L,$$

$$T_{23}(h^-) = \begin{cases} T_{23}(h^+), & |x|<L, \\ 0 & -a<x<-L, \ L<x<b, \end{cases}$$

$$T_{23}(-h) = 0 \quad -a<x<b. \tag{14a–f}$$

In addition, there are traction-free boundary conditions at the left and right edges of the plate:

$$T_{13} = 0, \quad x_1 = -a, b. \tag{14g}$$

For the transducer, the left and right edges are traction-free and are unelectroded and charge-free:

$$T_{13} = 0, \quad D_1 = 0, \quad x_1 = \pm L. \tag{14h}$$

4. Trigonometric series solution

We look for the solutions in the elastic plate and the transducer separately and then connect them by interface conditions. We use the complex notation. All fields are with an $\exp(i\omega t)$ factor which will be dropped for convenience.

4.1. The elastic plate

We consider the following field from separation of variables:

$$u = u(y)\left(\cos\frac{bn\pi}{a+b}\cos\frac{n\pi x}{a+b} + \sin\frac{bn\pi}{a+b}\sin\frac{n\pi x}{a+b}\right), \quad n = 1,2,3,\ldots\ . \tag{15}$$

Eq. (15) satisfies the edge conditions at $x=-a$ and b. Substitution of Eq. (15) into Eq. (3) results in

$$\frac{\partial^2 u}{\partial y^2} + \eta_n^2 u = 0, \tag{16}$$

where we have denoted

$$\eta_n = \left[\left(\frac{\omega}{c_2}\right)^2 - \left(\frac{n\pi}{a+b}\right)^2\right]^{1/2}. \tag{17}$$

Then the general solution for u can be written as

$$u = A_0\sin(\eta_0 y) + B_0\cos(\eta_0 y) + \sum_{n=1}^{\infty}[A_n\sin(\eta_n y) + B_n\cos(\eta_n y)]\left(\cos\frac{bn\pi}{a+b}\cos\frac{n\pi x}{a+b} + \sin\frac{bn\pi}{a+b}\sin\frac{n\pi x}{a+b}\right), \tag{18}$$

where A_n and B_n are undetermined constants. The following stress component is needed for boundary and continuity conditions:

$$T_{23} = \mu\eta_0 A_0 \cos(\eta_0 y) - \mu\eta_0 B_0 \sin(\eta_0 y) + \sum_{n=1}^{\infty}[\mu\eta_n A_n \cos(\eta_n y) - \mu\eta_n B_n \sin(\eta_n y)]\left(\cos\frac{bn\pi}{a+b}\cos\frac{n\pi x}{a+b} + \sin\frac{bn\pi}{a+b}\sin\frac{n\pi x}{a+b}\right). \tag{19}$$

4.2. The transducer

Consider the following modes from separation of variables [20]:

$$u = \begin{cases} U(y)\cos\dfrac{m\pi x}{2L}, & m = 2,4,6,\ldots \\ U(y)\sin\dfrac{m\pi x}{2L}, & m = 1,3,5,\ldots \end{cases}$$

$$\psi = \begin{cases} \Psi(y)\cos\dfrac{m\pi x}{2L}, & m = 2,4,6,\ldots \\ \Psi(y)\sin\dfrac{m\pi x}{2L}, & m = 1,3,5,\ldots \end{cases} \tag{20}$$

which already satisfy the edge conditions at $x_1 = \pm L$. Substitution of Eq. (22) into Eq. (11) results in

$$\frac{\partial^2 u}{\partial y^2} + \xi_m^2 u = 0, \quad \frac{\partial^2 \psi}{\partial y^2} - \left(\frac{m\pi}{2L}\right)^2 \psi = 0, \tag{21}$$

where

$$\xi_m = \left[\left(\frac{\omega}{v_T^2}\right)^2 - \left(\frac{m\pi}{2L}\right)^2\right]^{1/2}. \tag{22}$$

The general solution satisfying the transducer edge conditions can then be written as

$$u = F_0 \sin(\xi_0 y) + G_0 \cos(\xi_0 y) + \sum_{m=2,4,6,\ldots}^{\infty}[F_m \sin(\xi_m y) + G_m \cos(\xi_m y)]\cos\frac{m\pi x}{2L} + \sum_{m=1,3,5,\ldots}^{\infty}[F_m \sin(\xi_m y) + G_m \cos(\xi_m y)]\sin\frac{m\pi x}{2L},$$

$$\psi = H_0 y + K_0 + \sum_{m=2,4,6,\ldots}^{\infty}\left[H_m \sinh\frac{m\pi y}{2L} + K_m \cosh\frac{m\pi y}{2L}\right]\cos\frac{m\pi x}{2L} + \sum_{m=1,3,5,\ldots}^{\infty}\left[H_m \sinh\frac{m\pi y}{2L} + K_m \cosh\frac{m\pi y}{2L}\right]\sin\frac{m\pi x}{2L}, \tag{23}$$

where F_m, G_m, H_m and K_m are undetermined constants. The stress, electric displacement and electric potential needed for boundary conditions can be obtained as

$$\begin{aligned}\phi &= \psi + \frac{e}{\varepsilon}u \\ &= H_0 y + K_0 + \frac{e}{\varepsilon}F_0 \sin(\xi_0 y) + \frac{e}{\varepsilon}G_0 \cos(\xi_0 y) \\ &\quad + \sum_{m=2,4,6,\ldots}^{\infty}\left[\frac{e}{\varepsilon}F_m \sin(\xi_m y) + \frac{e}{\varepsilon}G_m \cos(\xi_m y) + H_m \sinh\frac{m\pi y}{2L} + K_m \cosh\frac{m\pi y}{2L}\right]\cos\frac{m\pi x}{2L} \\ &\quad + \sum_{m=1,3,5,\ldots}^{\infty}\left[\frac{e}{\varepsilon}F_m \sin(\xi_m y) + \frac{e}{\varepsilon}G_m \cos(\xi_m y) + H_m \sinh\frac{m\pi y}{2L} + K_m \cosh\frac{m\pi y}{2L}\right]\sin\frac{m\pi x}{2L},\end{aligned} \tag{24}$$

$$
\begin{aligned}
T_{23} &= \bar{c}u_{,2} + e\psi_{,2} \\
&= \bar{c}\xi_0 F_0 \cos(\xi_0 y) - \bar{c}\xi_0 G_0 \sin(\xi_0 y) + eH_0 \\
&\quad + \sum_{m=2,4,6,\cdots}^{\infty} \Big[\bar{c}\xi_m F_m \cos(\xi_m y) - \bar{c}\xi_m G_m \sin(\xi_m y) \\
&\quad + e\frac{m\pi}{2L} H_m \cosh\frac{m\pi y}{2L} + e\frac{m\pi}{2L} K_m \sinh\frac{m\pi y}{2L}\Big] \cos\frac{m\pi x}{2L} \\
&\quad + \sum_{m=1,3,5,\ldots}^{\infty} \Big[\bar{c}\xi_m F_m \cos(\xi_m y) - \bar{c}\xi_m G_m \sin(\xi_m y) \\
&\quad + e\frac{m\pi}{2L} H_m \cosh\frac{m\pi y}{2L} + e\frac{m\pi}{2L} K_m \sinh\frac{m\pi y}{2L}\Big] \sin\frac{m\pi x}{2L},
\end{aligned} \tag{25}
$$

$$
\begin{aligned}
D_2 = -\varepsilon\psi_{,2} &= -\varepsilon H_0 + \sum_{m=2,4,6,\ldots}^{\infty} \Big[-\varepsilon\frac{m\pi}{2L} H_m \cosh\frac{m\pi y}{2L} - \varepsilon\frac{m\pi}{2L} K_m \sinh\frac{m\pi y}{2L}\Big] \cos\frac{m\pi x}{2L} \\
&\quad + \sum_{m=1,3,5,\ldots}^{\infty} \Big[-\varepsilon\frac{m\pi}{2L} H_m \cosh\frac{m\pi y}{2L} - \varepsilon\frac{m\pi}{2L} K_m \sinh\frac{m\pi y}{2L}\Big] \cos\frac{m\pi x}{2L}.
\end{aligned} \tag{26}
$$

4.3. Boundary and continuity conditions

Substituting Eqs. (24)–(26) into Eqs. (14a)–(14d), we obtain

$$
\begin{aligned}
&H_0(h+2h') + K_0 + \frac{e}{\varepsilon} F_0 \sin(\xi_0(h+2h')) + \frac{e}{\varepsilon} G_0 \cos(\xi_0(h+2h')) \\
&\quad + \sum_{m=2,4,6,\ldots}^{\infty} \Big[\frac{e}{\varepsilon} F_m \sin(\xi_m(h+2h')) + \frac{e}{\varepsilon} G_m \cos(\xi_m(h+2h')) \\
&\quad + H_m \sinh\frac{m\pi(h+2h')}{2L} + K_m \cosh\frac{m\pi(h+2h')}{2L}\Big] \cos\frac{m\pi x}{2L} \\
&\quad + \sum_{m=1,3,5,\ldots}^{\infty} \Big[\frac{e}{\varepsilon} F_m \sin(\xi_m(h+2h')) + \frac{e}{\varepsilon} G_m \cos(\xi_m(h+2h')) \\
&\quad + H_m \sinh\frac{m\pi(h+2h')}{2L} + K_m \cosh\frac{m\pi(h+2h')}{2L}\Big] \sin\frac{m\pi x}{2L} = V,
\end{aligned} \tag{27}
$$

$$
\begin{aligned}
&\bar{c}\xi_0 F_0 \cos(\xi_0(h+2h')) - \bar{c}\xi_0 G_0 \sin(\xi_0(h+2h')) + eH_0 \\
&\quad + \sum_{m=2,4,6,\ldots}^{\infty} \Big[\bar{c}\xi_m F_m \cos(\xi_m(h+2h')) - \bar{c}\xi_m G_m \sin(\xi_m(h+2h')) \\
&\quad + e\frac{m\pi}{2L} H_m \cosh\frac{m\pi(h+2h')}{2L} + e\frac{m\pi}{2L} K_m \sinh\frac{m\pi(h+2h')}{2L}\Big] \cos\frac{m\pi x}{2L} \\
&\quad + \sum_{m=1,3,5,\ldots}^{\infty} \Big[\bar{c}\xi_m F_m \cos(\xi_m(h+2h')) - \bar{c}\xi_m G_m \sin(\xi_m(h+2h')) \\
&\quad + e\frac{m\pi}{2L} H_m \cosh\frac{m\pi(h+2h')}{2L} + e\frac{m\pi}{2L} K_m \sinh\frac{m\pi(h+2h')}{2L}\Big] \sin\frac{m\pi x}{2L} = 0,
\end{aligned} \tag{28}
$$

$$
\begin{aligned}
&H_0(h) + K_0 + \frac{e}{\varepsilon} F_0 \sin(\xi_0 h) + \frac{e}{\varepsilon} G_0 \cos(\xi_0 h) \\
&\quad + \sum_{m=2,4,6,\ldots}^{\infty} \Big[\frac{e}{\varepsilon} F_m \sin(\xi_m h) + \frac{e}{\varepsilon} G_m \cos(\xi_m h) + H_m \sinh\frac{m\pi h}{2L} + K_m \cosh\frac{m\pi h}{2L}\Big] \cos\frac{m\pi x}{2L}
\end{aligned}
$$

$$+\sum_{m=1,3,5,\ldots}^{\infty}\left[\frac{e}{\varepsilon}F_m\sin(\xi_m h)+\frac{e}{\varepsilon}G_m\cos(\xi_m h)+H_m\sinh\frac{m\pi h}{2L}+K_m\cosh\frac{m\pi h}{2L}\right]\sin\frac{m\pi x}{2L}=-V, \tag{29}$$

$$\begin{aligned}&A_0\sin(\eta_0 h)+B_0\cos(\eta_0 h)\\&+\sum_{n=1}^{\infty}[A_n\sin(\eta_n h)+B_n\cos(\eta_n h)]\left(\cos\frac{bn\pi}{a+b}\cos\frac{n\pi x}{a+b}+\sin\frac{bn\pi}{a+b}\sin\frac{n\pi x}{a+b}\right)\\&=F_0\sin(\xi_0 h)+G_0\cos(\xi_0 h)+\sum_{m=2,4,6,\ldots}^{\infty}[F_m\sin(\xi_m h)+G_m\cos(\xi_m h)]\cos\frac{m\pi x}{2L}\\&+\sum_{m=1,3,5,\ldots}^{\infty}[F_m\sin(\xi_m h)+G_m\cos(\xi_m h)]\sin\frac{m\pi x}{2L},\end{aligned} \tag{30}$$

which are to be multiplied by $\cos p\pi x/2L$ or $\sin p\pi x/2L$ and integrated from $-L$ to L for $p=0, 2, 4,\ldots$ and $p=1, 3, 5,\ldots$, respectively, so that linear algebraic equations of the undetermined coefficients will result. Substitution of Eqs. (24)–(26) into Eqs. (14e)–(14f) gives

$$\begin{aligned}&\mu\eta_0 A_0\cos(\eta_0 h)-\mu\eta_0 B_0\sin(\eta_0 h)\\&+\sum_{n=1}^{\infty}[\mu\eta_n A_n\cos(\eta_n h)-\mu\eta_n B_n\sin(\eta_n h)]\left(\cos\frac{bn\pi}{a+b}\cos\frac{n\pi x}{a+b}+\sin\frac{bn\pi}{a+b}\sin\frac{n\pi x}{a+b}\right)\\&=\overline{c}\xi_0 F_0\cos(\xi_0 h)-\overline{c}\xi_0 G_0\sin(\xi_0 y)+eH_0+\sum_{m=2,4,6,\cdots}^{\infty}\left[\overline{c}\xi_m F_m\cos(\xi_m h)-\overline{c}\xi_m G_m\sin(\xi_m h)\right.\\&\left.+e\frac{m\pi}{2L}H_m\cosh\frac{m\pi h}{2L}+e\frac{m\pi}{2L}K_m\sinh\frac{m\pi h}{2L}\right]\cos\frac{m\pi x}{2L}\\&+\sum_{m=1,3,5,\ldots}^{\infty}\left[\overline{c}\xi_m F_m\cos(\xi_m h)-\overline{c}\xi_m G_m\sin(\xi_m h)\right.\\&\left.+e\frac{m\pi}{2L}H_m\cosh\frac{m\pi h}{2L}+e\frac{m\pi}{2L}K_m\sinh\frac{m\pi h}{2L}\right]\sin\frac{m\pi x}{2L}\quad\text{for } |x|<L,\\0\quad&\text{for } -a<x<-L,\ \ L<x<b.\end{aligned} \tag{31}$$

$$\begin{aligned}&\mu\eta_0 A_0\cos(\eta_0 h)+\mu\eta_0 B_0\sin(\eta_0 h)+\sum_{n=1}^{\infty}[\mu\eta_n A_n\cos(\eta_n h)\\&+\mu\eta_n B_n\sin(\eta_n h)]\left(\cos\frac{bn\pi}{a+b}\cos\frac{n\pi x}{a+b}+\sin\frac{bn\pi}{a+b}\sin\frac{n\pi x}{a+b}\right)=0\end{aligned} \tag{32}$$

which are to be multiplied by

$$\cos\frac{bp\pi}{a+b}\cos\frac{p\pi x}{a+b}+\sin\frac{bp\pi}{a+b}\sin\frac{p\pi x}{a+b} \tag{33}$$

and integrated from $-a$ to b for $p=1, 2, 3,\ldots$.

5. Numerical results

As a numerical example, consider a transducer made from polarized ceramics PZT-5H [21]. For PZT-5H, we have $\rho=7500\,\mathrm{kg/m^3}$, $c_{44}=2.30\times10^{10}\,\mathrm{N/m^2}$, $e_{15}=17\,\mathrm{C/m^2}$ and $\varepsilon_{11}=1.505\times10^{-8}\,\mathrm{C/Vm}$. Damping is introduced by allowing the elastic constant of the ceramics c_{44} to assume complex values, which can represent viscous damping in the material. In our calculations, c_{44} is replaced by $c_{44}(1+\mathrm{i}Q^{-1})$ where Q is a large and real number. Similarly, for the elastic shell, μ is replaced by $\mu(1+\mathrm{i}Q^{-1})$. In reality, different materials have

different values of Q. We will use the same Q as a single damping parameter of the whole system. For polarized ceramics, the value of Q is of the order of 10^2–10^3. We fix $Q = 20$ which is relatively large and is considered as a measure of all the damping in the whole structure. For the elastic layer, we consider steel with $\rho_1 = 7850\,\mathrm{kg/m^3}$ and $\mu = 80 \times 10^9\,\mathrm{N/m^2}$. We fix $a = b = 10L = 0.5\,\mathrm{m}$, $h = 0.01\,\mathrm{m}$ and $V = 220\,\mathrm{V}$. We use the following frequency ω_0 as a normalizing frequency which is the fundamental pure thickness-twist frequency of the elastic plate when the actuator is not present:

$$\omega_0^2 = \frac{\mu\pi^2}{\rho_1(2h)^2}. \tag{34}$$

Fig. 2 shows the displacement (real part) of the middle point of the upper surface of the elastic plate versus the driving frequency. At certain frequencies the displacement becomes large (resonance).

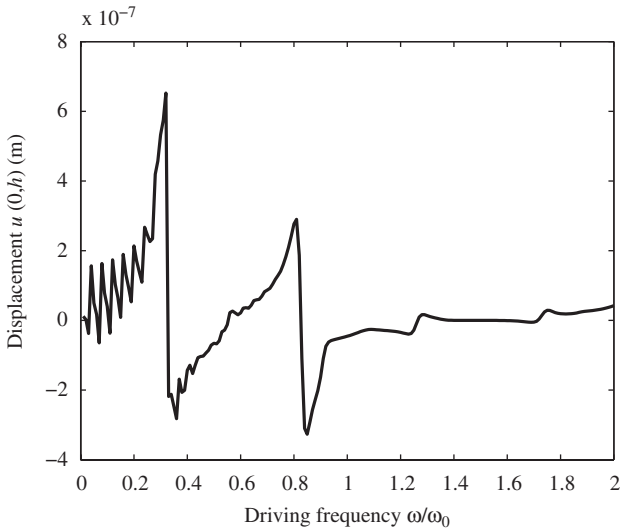

Fig. 2. $u(0,h)$ versus driving frequency ($h' = h$).

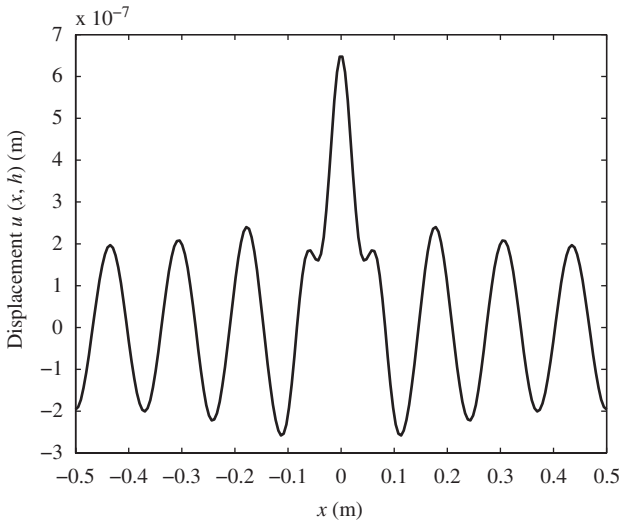

Fig. 3. Distribution of $u(x,h)$ at the first resonance ($h' = h$, $a = b$, $\omega = 0.32\omega_0$).

In Figs. 3–6 we have plot the displacement (real part) distribution along the upper surface of the elastic plate for the first four resonances. Shear horizontal (SH) modes in an elastic plate are called face-shear and thickness-twist modes according to Refs. [22,23]. The one with the lowest frequency is called the face-shear wave which does not vary long the plate thickness and is called a symmetric mode. All the higher order modes are called thickness-twist waves with variation and nodal points along the plate thickness and can be symmetric or anti-symmetric about the middle plane of the elastic plate. Since the excitation is on one side of the plate only, symmetric and anti-symmetric modes are all excited. Depending on the driving frequency, certain modes may dominate. Thickness-twist modes have cutoff frequencies below which they cannot propagate and the waves die out in the x direction. However, the face-shear wave does not have a cutoff frequency and can always propagate. As combinations of face-shear and thickness-twist waves, Figs. 3–6 sometimes show vibrations essentially confined under or close to the piezoelectric actuator, or essentially all over the plate. These are useful for

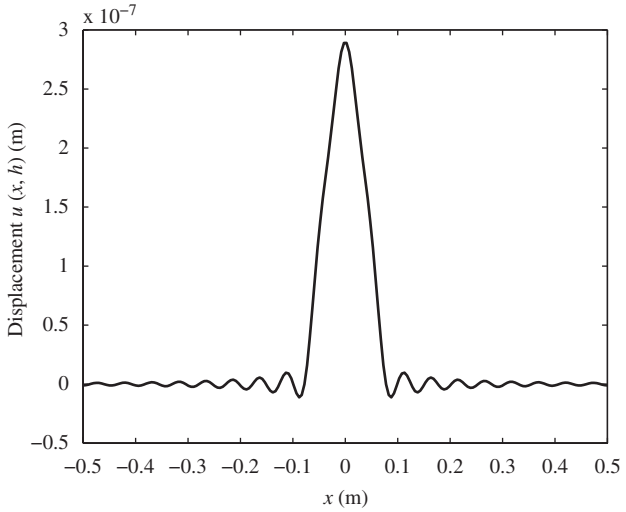

Fig. 4. Distribution of $u(x,h)$ at the second resonance ($h' = h$, $a = b$, $\omega = 0.81\omega_0$).

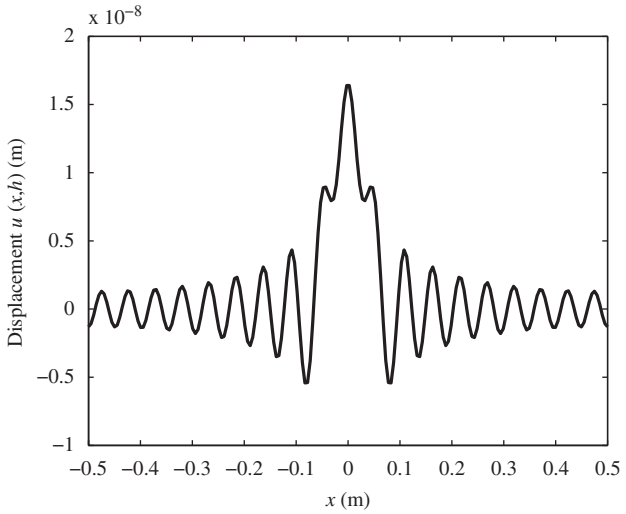

Fig. 5. Distribution of $u(x,h)$ at the third resonance ($h' = h$, $a = b$, $\omega = 1.28\omega_0$).

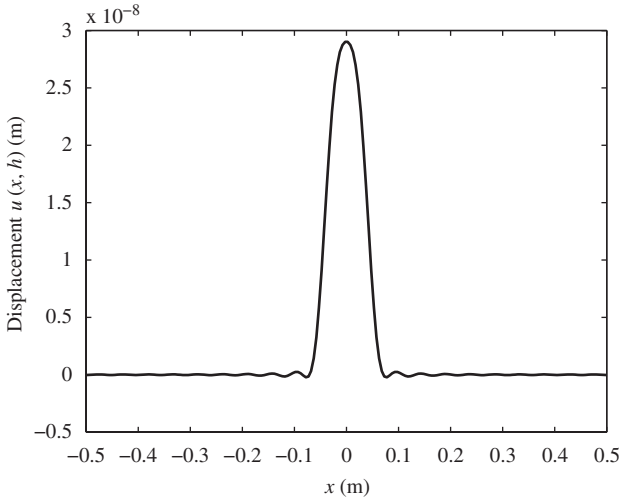

Fig. 6. Distribution of $u(x,h)$ at the fourth resonance ($h' = h$, $a = b$, $\omega = 1.75\omega_0$).

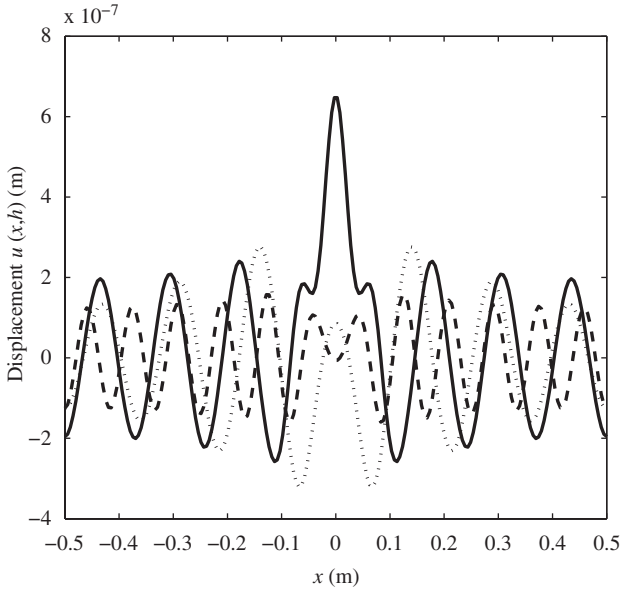

Fig. 7. Distribution of $u(x,h)$ at the first resonance for different actuator thickness ($a = b$). Solid line: $\omega = 0.32\omega_0$, $h' = h$; dashed line: $\omega = 0.48\omega_0$, $h' = 0.5h$; dotted line: $\omega = 0.26\omega_0$, $h' = 1.5h$.

different applications. For example, in non-destructive evaluation we need modes that can feel the entire plate. Then no matter where a defect is the resonant frequency or the electric admittance is affected. There are also other applications in which vibration confined to a local area is desired (called energy trapping).

In Fig. 7 we show the effect of different actuator thickness on the vibration at the first resonance. Both the resonant frequency and vibration distribution are sensitive to the actuator thickness. Fig. 8 presents the electric admittance versus the driving frequency. Near a resonance the admittance assumes maximum because at a resonance the deformation is large, resulting in more charges through piezoelectric coupling and a large current on the electrodes.

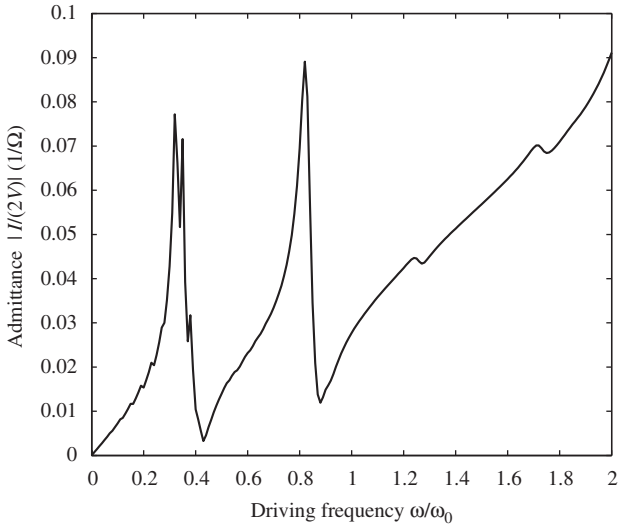

Fig. 8. Admittance versus driving frequency ($h' = h$, $a = b$).

6. Conclusion

A trigonometric series solution is obtained for shear-horizontal vibrations of an elastic plate with a finite piezoelectric actuator. The solution satisfies the equations of elasticity and piezoelectricity. Numerical results show that coupled face-shear and thickness-twist modes are excited in the plate. The vibration may be confined to the actuator region (energy trapping) or all over the elastic plate. This difference is important to various applications depending on whether local or global vibration is desired. The vibration distribution is sensitive to the actuator thickness and the electric admittance becomes large at resonances. The results are useful in acoustic wave devices and nondestructive evaluation.

Acknowledgments

This work was supported by the National Natural Science Foundation of China through Grant #50778179. The first author was supported by a scholarship from the Ministry of Education of China as a visiting student to the University of Nebraska.

References

[1] X.Q. He, T.Y. Ng, S. Sivashanker, K.M. Liew, Active control of FGM plates with integrated piezoelectric sensors and actuators, *International Journal of Solids and Structures* 38 (9) (2001) 1641–1655.

[2] K.M. Liew, X.Q. He, T.Y. Ng, S. Kitipornchai, Finite element piezothermoelasticity analysis and the active control of FGM plates with integrated piezoelectric sensors and actuators, *Computational Mechanics* 31 (3–4) (2003) 350–358.

[3] K.M. Liew, J.Z. Zhang, T.Y. Ng, S.A. Meguid, Three-dimensional modelling of elastic bonding in composite laminates using layerwise differential quadrature, *International Journal of Solids and Structures* 40 (7) (2003) 1745–1764.

[4] K.M. Liew, J.Z. Zhang, C. Li, S.A. Meguid, Three-dimensional analysis of the coupled thermo-piezoelectro-mechanical behaviour of multilayered plates using the differential quadrature technique, *International Journal of Solids and Structures* 42 (14) (2005) 4239–4257.

[5] J.Z. Zhang, T.Y. Ng, K.M. Liew, Three-dimensional theory of elasticity for free vibration analysis of composite laminates via layerwise differential quadrature modelling, *International Journal of Numerical Methods Engineering* 57 (13) (2003) 1819–1844.

[6] K.M. Liew, J.Z. Zhang, T.Y. Ng, J.A. Reddy, Dynamic characteristics of elastic bonding in composite laminates: a free vibration study, *Journal of Applied Mechanics—Transactions of the ASME* 70 (6) (2003) 860–870.

[7] K.M. Liew, X.Q. He, M.J. Tan, H.K. Lim, Dynamic analysis of laminated composite plates with piezoelectric sensor/actuator patches using the FSDT mesh-free method, *International Journal of Mechanical Sciences* 46 (3) (2004) 411–431.

[8] J.S. Yang, R.C. Batra, X.Q. Liang, The cylindrical bending vibration of a laminated elastic plate due to piezoelectric actuators, *Smart Materials and Structures* 3 (1994) 485–493.
[9] R.C. Batra, X.Q. Liang, J.S. Yang, The vibration of a simply supported rectangular elastic plate due to piezoelectric actuators, *International Journal of Solids and Structures* 33 (1996) 1597–1618.
[10] W.Q. Chen, R.Q. Xu, H.J. Ding, On free vibration of a piezoelectric composite rectangular plate, *Journal of Sound and Vibration* 218 (1998) 741–748.
[11] Z. Zhang, C. Feng, K.M. Liew, Three-dimensional vibration analysis of multilayered piezoelectric composite plates, *International Journal of Engineering Science* 44 (2006) 397–408.
[12] J.X. Gao, Y.P. Shen, J. Wang, Three dimensional analysis for free vibration of rectangular composite laminates with piezoelectric layers, *Journal of Sound and Vibration* 213 (1998) 383–390.
[13] C.K. Lee, Theory of laminated piezoelectric plates for the design of distributed sensors/actuators, Part I: governing equations and reciprocal relationships, *Journal of the Acoustical Society of America* 87 (3) (1990) 1144–1158.
[14] E.K. Dimitriadis, C.R. Fuller, C.A. Rogers, Piezoelectric actuators for distributed vibration excitation of thin plates, *Journal of Vibration and Acoustics* 113 (1991) 100–107.
[15] H.F. Tiersten, Equations for the control of the flexural vibrations of composite plates by partially electroded piezoelectric actuators, in: G.L. Anderson, D.C. Lagoudas, (Eds.), *Proceedings of the Active Materials and Smart Structures Conference*, College Station, TX, USA, October 1994, *SPIE Proceedings* 2427, 1994, pp. 326–342.
[16] J.S. Yang, Equations for elastic plates with partially electroded piezoelectric actuators in flexure with shear deformation and rotatory inertia, *Journal of Intelligent Material Systems and Structures* 8 (1997) 444–451.
[17] B.X. Zhang, C.H. Wang, A. Bostrom, Study of acoustic radiation field excited by a piezoelectric strip, *Acta Physica Sinica* 54 (2005) 2111–2116 (in Chinese).
[18] J.L. Bleustein, A new surface wave in piezoelectric materials, *Applied Physics Letters* 13 (1968) 412–413.
[19] J.L. Bleustein, Some simple modes of wave propagation in an infinite piezoelectric plate, *The Journal of Acoustical Society of America* 45 (1969) 614–620.
[20] J.S. Yang, S.H. Guo, Thickness-twist modes in a rectangular piezoelectric resonator of hexagonal crystals, *Applied Physics Letters* 88 (15) (2006) Art. No. 153506.
[21] H. Jaffe, D.A. Berlincourt, Piezoelectric transducer materials, *Proceedings of IEEE* 53 (1965) 1372–1386.
[22] R.D. Mindlin, Face-shear waves in rotated Y-cut quartz plates, in: F.P.J. Rimrott, J. Schwaighofer (Eds.), *Mechanics of the Solid State*, University of Toronto Press, 1968, pp. 143–145.
[23] R.D. Mindlin, Thickness-twist vibrations of an infinite, monoclinic, crystal plate, *International Journal of Solids Structures* 1 (1965) 141–145.